Study on the Method for Detecting and Monitoring of Pre-Failure Deformation in Slope

Kiminori Araiba
National Research Institute of Fire and Disaster, Jindaiji-Higashimachi 4-35-3, Chofu, Tokyo 182-8508, Japan (araiba@fri.go.jp)

Abstract

In order to develop a technique for remotely monitoring deformation of slope before the failure, a method of repeated surveying of the surface using a laser scanner set on the ground was studied. The accuracy of measurement was verified by a laboratory test and spatial stacking was proposed to suppress the effect of errors in measurement on the calculation of deformation.

The method was applied to failure experiments carried out on a model slope (5 m in height, 1 m in depth and 30° in inclination). The data revealed the distribution of deformation on the slope and its time variation. Subsidence and retreat of the surface's upper region and the uplift and advance of surface in its lower region were recognized approximately 30 minutes before the failure. Areas of each deformation enlarged with time. The amount of deformation was up to 0.2 m and acceleration was observed in some segments of the slope. Data obtained using this method revealed time dependent characteristics of pre-failure slope deformation.

The measuring technique was applied to an actual slope failure. The scarp of slope failure was surveyed twice with an interval of one month using a long-range-type laser scanner. Displacement of a rock separated from a scarp by cracks was detected. It is clarified that density of data is important to calculate precise deformation.

Keywords: slope failure, landslide, deformation, monitoring, remote sensing

Introduction

Assessing and controlling the risk of a secondary disaster during a search and rescue (S&R) operation at a disaster site are difficult because both the quantity and quality of information regarding the disaster are usually inadequate due to the limited time and space available for investigation. As one example, sixty fire-fighting volunteers were killed during an S&R activity because of a secondary failure of a slope that occurred approximately four hours after the initial slope failure, which had buried one person in Shigeto, Kochi prefecture, Japan, in 1972 (Nakagawa and Okunishi (1977).

An intensive S&R activity was undertaken in a slope failure at Myoken, Nagaoka city triggered by Niigataken-Chuetsu Earthquake on 23 October 2004. It started at noon on 26 October and finished in the afternoon of 28 October. In this case, experts from the Public Work Research Institute conducted aerial and ground investigations, then identified the risk factors. They suggested a mitigation plan that included target areas to be watched, arrangement of watchmen, and an action plan for each member in the case of an emergency. This effort led the activity to safe completion and was highly appreciated by rescue crews (Ebisawa (2005)).

The author was dispatched to the rescue site at midnight after experts from the PWRI completed their intensive half-day-long work. During the activity, the author realized the necessity of automatic monitoring because visual monitoring seemed ineffective due to darkness, large dead angles, decrease in the concentration levels of watchmen over time and the bluntness of the human senses in detecting slow movements.

Extensometers are frequently used in the field of slope failure. Saito and Uezawa (1961) first discussed the time prediction of failure using extensometer data; related studies have been carried out (e.g., Varnes (1982), Fukuzono (1985), Hayashi and Yamamori (1991)). An extensometer is easy to set up, and it provides one-dimensional data; therefore, it is easy to handle. On the other hand, it has the following drawbacks:

1) It measures the variation in the distance between two posts. One post must be located on the stable ground and the other on the potential failure mass. However, it is difficult to recognize the failure part and stable part before failure actually occurs, especially in cases in which numerous cracks exist on the slope.

2) The installation must be carried out in an unstable area.

pp. 581–589

Table 1. Specifications of equipments used in this study.

Target	Name of equipment	Precision of distance measuring	Resolution of angle control	Beam divergence	Scanning speed
Model slope	LPM-25HA	8 mm	0.009°	1.2mrad	1000 points / sec.
Scarp of Myoken	LPM-2K	50 mm	0.009°	1.2mrad	4 points / sec.

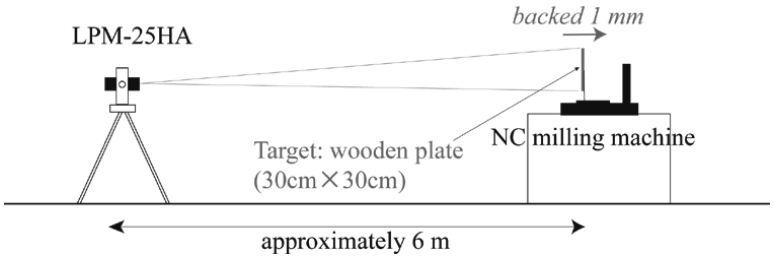

Fig. 1. Schematic arrangement for the test for the accuracy of measurement.

3) The direction of movement of the sliding mass is not always parallel to the direction of the extensometer's sensitivity.

By means of repeated surveying, it is possible to monitor the spatial distribution of the deformation on a certain extent of the slope; therefore, defects 1 and 3 can be overcome. With regard to defect 2, some survey methods require no targets, such as use of laser scanners, photographic measurements, and fringe analyses. These methods can reveal three-dimensional deformations that can provide information for understanding the mechanism of a potential failure. The application of such a method to monitoring of a slope failure can allow the monitoring to start quickly and safely, which are the desirable qualities of an emergency response.

In this study, availability of repeated surveying using a laser scanner installed on the ground for monitoring pre-failure deformation of slope was investigated by means of an accuracy test, model slope experiments and a field investigation. The laser scanner measures distance to a part of a target that lies within the angular width of the laser pulse beam divergence, and it automatically scans the designated vertical and horizontal angle widths by using designated angle intervals. The accuracy of the laser scanner is not as good as that of a total station; however, it can quickly measure wide areas. The accuracy of measurement was checked by a test in a laboratory and a method for compressing errors was suggested. The survey technique was then applied to three failure experiments on a model slope to verify the possibility of detecting pre-failure deformation. To check the ability of monitoring in a real topography, the scarp of the slope failure in Myoken was surveyed using a long-range laser scanner twice with an interval of one month. Specifications of laser scanners used in this study are listed in Table 1.

Accuracy test

Figure 1 shows the schematic arrangement for the test for determining the measurement accuracy. A wooden plate was held by an NC milling machine set at a distance of about 6 m from the laser scanner. The plate was measured by the scanner in its initial position and then displaced by 1.00 mm by the milling machine and measured again.

Figure 2 shows the frequency distribution of the distance between the wooden plate and the vertical plane on which the laser scanner was situated, which is parallel to the wooden plate. The average value is 0.00108 m, which is consistent with the real value. A certain portion of the data showed a significant positive and negative difference. Multiple reflections can be considered as the most probable cause for them because the target was in close proximity to the scanner and the wooden plate is a good reflector. The standard deviation was 0.0034 m.

Stacking of data is one of methods to improve the measurement accuracy. Because the time available in an emergency situation is generally limited, stacking along the time axis is not suitable in this case and spatial averaging is preferable. It will be described in the subsequent "Data processing" section.

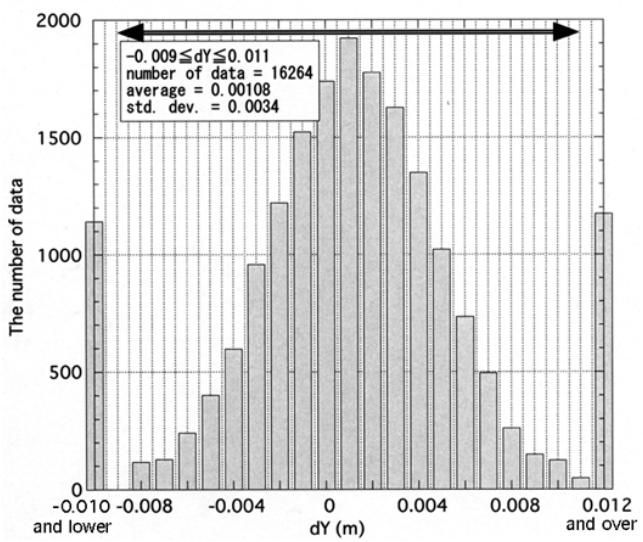

Fig. 2. Frequency distribution of measured displacement of wooden plate.

Table 2. Conditions of measurements.

Target	Minimum distance	Horizontal angular width	Horizontal angular step	Vertical angular width	Vertical angular step	Time for one scan	Approximate number of data
Model slope experiment 1	12.0 m	21.6°	0.108 °	18.0°	0.054°	4 min.	35000
Model slope experiment 2	10.5 m	20.6°	0.198 °	17.0 °	0.099 °	1.5 min.	13500
Model slope experiment 3	16.5 m	26.2°	0.153 °	17.0 °	0.099 °	2.4 min.	14000
Scarp of Myoken, Nov. 7th	560 m	4.770°	0.027°	1.845°	0.027°	110 min.	12000
Scarp of Myoken, Dec. 7th	550 m	4.392°	0.027 °	2.214°	0.027 °	70 min.	10000

Failure experiment of a model slope

Experiments involving model slope failure induced by artificial rainfall were performed in the large-scale rainfall simulator at the National Research Institute for Earth Science and Disaster Prevention (Fukuzono and Terasawa (1985)).

A model slope covered by a soil layer with a height of 5 m, width of 4 m, depth of 1 m and an inclination of 30 ° was constructed using river sand. Water was sprayed from nozzles that were set at a 6-m-high ceiling. A series of preparatory sprays were applied to the model slope for about 10 days. Each preparatory spray application was done for 8 h per day; its intensity was increased on a daily basis from 15 mm/h to 45 mm/h. On the final day, the intensity was increased to 50 mm/h, and water was sprayed until the model slope eventually failed. Three experiments were conducted. In experiment 1, water was allowed to seep from the bottom of the soil layer. In experiments 2 and 3, no seepage was allowed. Figure 3 shows photographs of the model slope before and after the failure.

Measurement conditions are listed in Table 2. The laser scanner was placed on a tripod stand on the ground. In experiments 1 and 2, it was placed in front of the model slope. In experiment 3, it was placed in an oblique direction approximately 7° from the nodal line of the model slope.

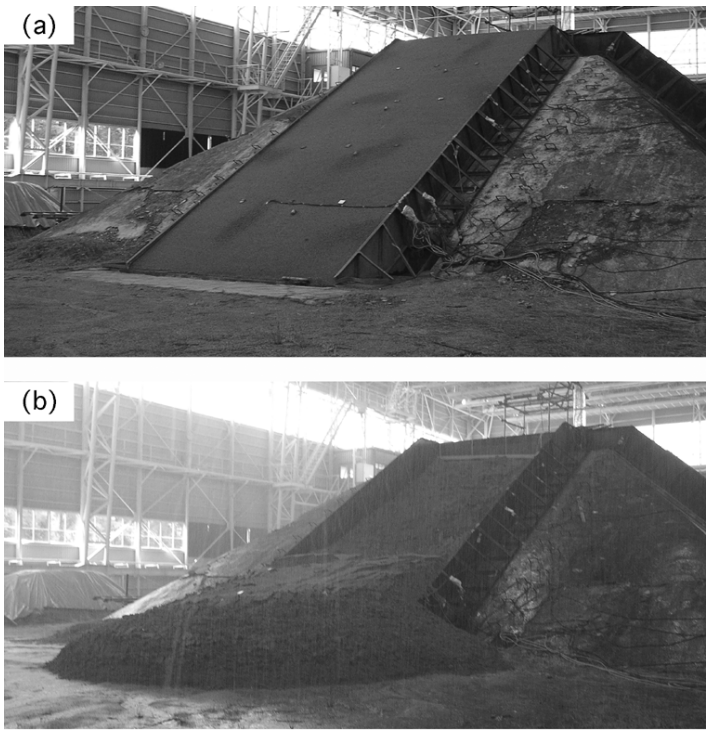

Fig. 3. Photographs of model slope: (a) before the collapse, (b) after the collapse.

Data processing

The obtained data were converted to Cartesian coordinates. The directions of the axes were fixed as shown in Figure 4; the Z-axis is aligned in the vertical direction, the Y-axis is along the macroscopically longitudinal direction of the slope in the horizontal plane, and the X-axis is along the macroscopically transverse direction. X = 0 represents the slope centre; Y = 0, the plane on which the laser scanner is mounted; and Z = 0, the bottom of the slope.

The collected data were then processed as follows:

1) Isolated points in the air were eliminated because they were easily recognized as errors. This function was realized by automatically eliminating the data that resulted in a steep overhang.
2) Data points were projected onto the X–Y plane.
3) Meshes with 0.1 m width were applied on the plane.
4) The Z values of all the points inside each mesh were averaged to give the representative Z value of that mesh.
5) The difference in the representative value between the initial state and each measurement was calculated for each mesh.
6) The result of 5) was plotted on the X–Y plane, thus providing the distribution of deformation along the vertical direction at the time of each measurement.
7) The same procedure was performed for calculating the distribution of deformation along the Y direction on the X–Z plane.

Process 4) represents data stacking mentioned in the section "Accuracy test" section. Assuming that N observed points are scattered randomly within each mesh, the amount of the expected standard deviation of the representative value, which is calculated by averaging over the observed points, would be $1/\sqrt{N}$ of that of an individual point. Therefore, the expected value of the standard deviation of the representative values for the meshes is considered to be from 0.0017 m (deformation in Z direction in experiment 2) to 0.0007 m (deformation in Y in experiment 1). In the following sections, data obtained for experiment 2 will be used.

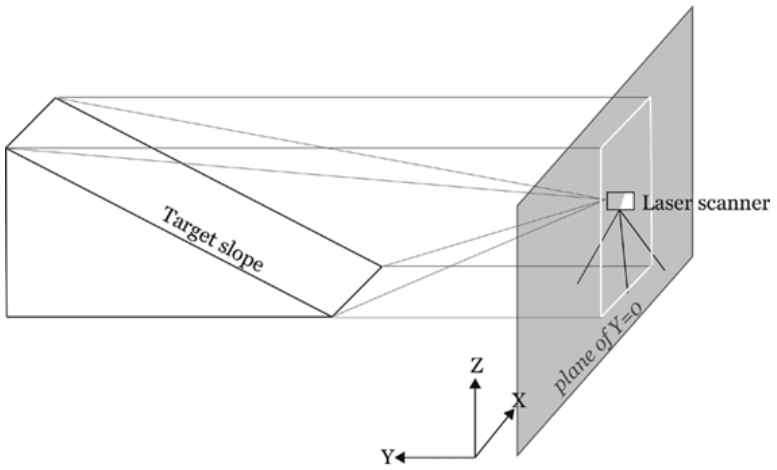

Fig. 4. Definition of coordinate system.

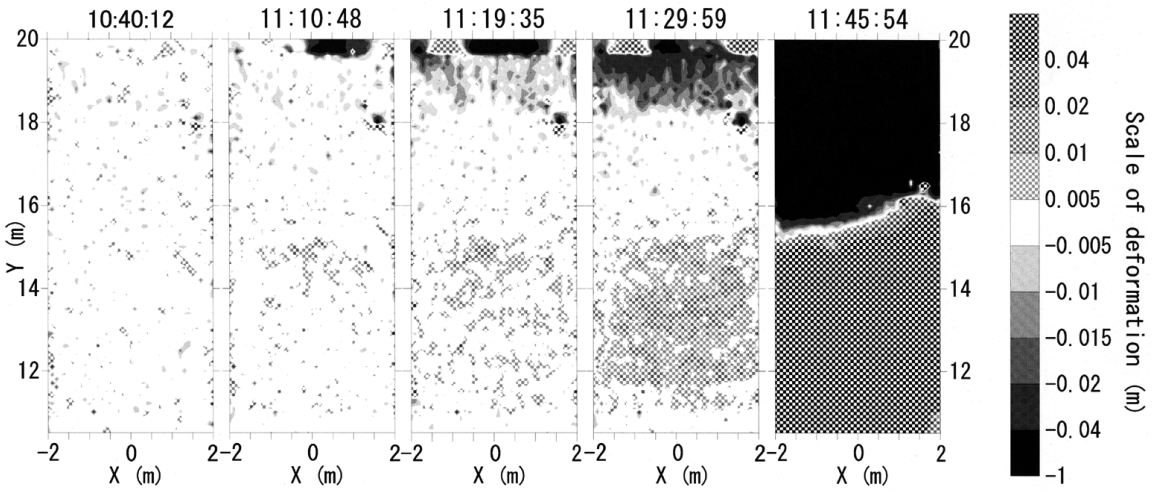

Fig. 5. Distribution of deformation along the Z direction projected onto the X–Y plane in model slope experiment 2. The time at which each measurement was performed is indicated above each diagram; the original measurement was performed at 10:38:45.

Result of model slope failure

Spatial distribution of deformation

Figure 5 shows the variation in the distribution of deformation along the Z direction projected onto the horizontal plane in experiment 2. The result of measurement at 10:38:45 was used as the initial shape. It was subtracted from the result of each measurement at the time noted above each diagram. The time indicates the start time of the measurement recorded by the PC. The failure occurred at about 11:45:00: the diagram for 11:45:54 shows a topographic change before and after the failure. A positive value indicates uplift, whereas a negative value indicates subsidence. In the diagram for 10:40:12, a small deformation is visible. Considering that 87 s is a short period, this diagram can be interpreted as an example of the error that is inherent in the method used in this study. The amount of deformation increases with time. Comparing the diagram for 11:19:35 to that for 10:40:12, it can be concluded that deformation can be detected prior to failure. In the diagram for 11:10:48, a small amount of uplift can be observed in the middle section of the slope; it increases with time in its spread as well as its amount. Subsidence is detected on the most distant area of the slope. It increases monotonously in both area and amount.

Figure 6 shows the variation in distribution of deformation along the Y direction. A positive value indicates retrogressing, whereas a negative value indicates swelling. In the diagram for 11:10:48, an area with retrogressive deformation and another with swelling are visible at the top and middle (Z = 2) of the slope,

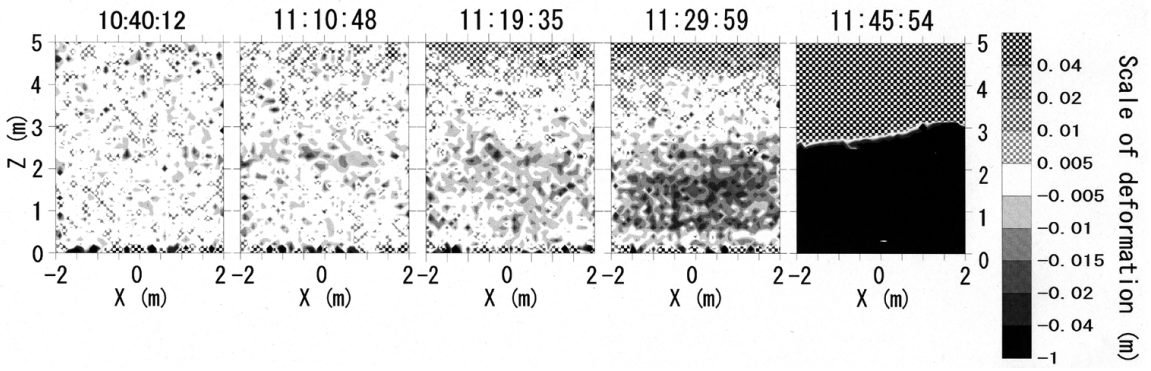

Fig. 6. Distribution of deformation along the Y direction projected onto the X–Z plane in model slope experiment 2. The time at which each measurement was performed is indicated above each diagram; the original measurement was performed at 10:38:45.

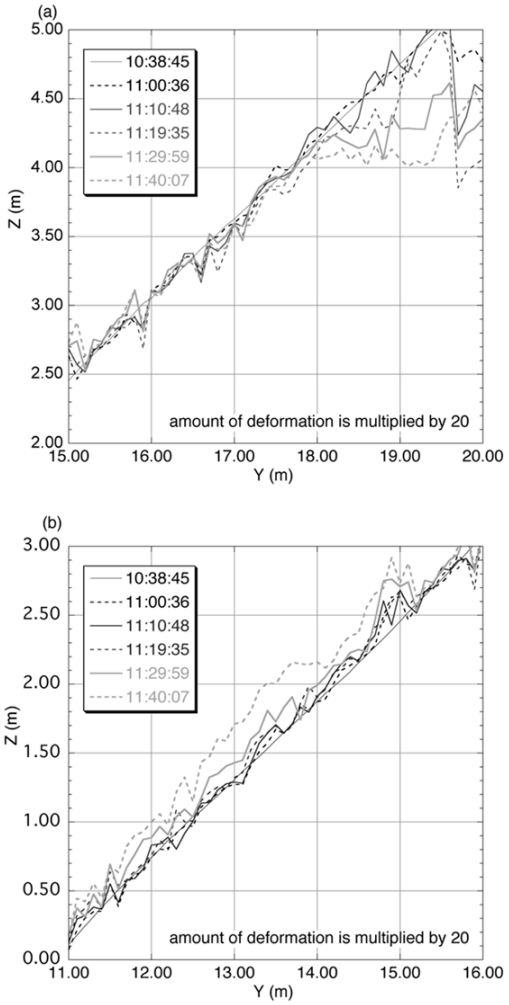

Fig. 7. Change of longitudinal section of the slope centre. Deformation amount is enlarged 20 times.

respectively. The area and amount of each deformation increase with time.

These figures clarify that the amount and spatial distribution of deformation before the failure are revealed by this method under the conditions of a model experiment. Furthermore, it may be possible to estimate the failed section of the slope as a segment between a subsiding (retrogressing) area and a heaving (swelling) area.

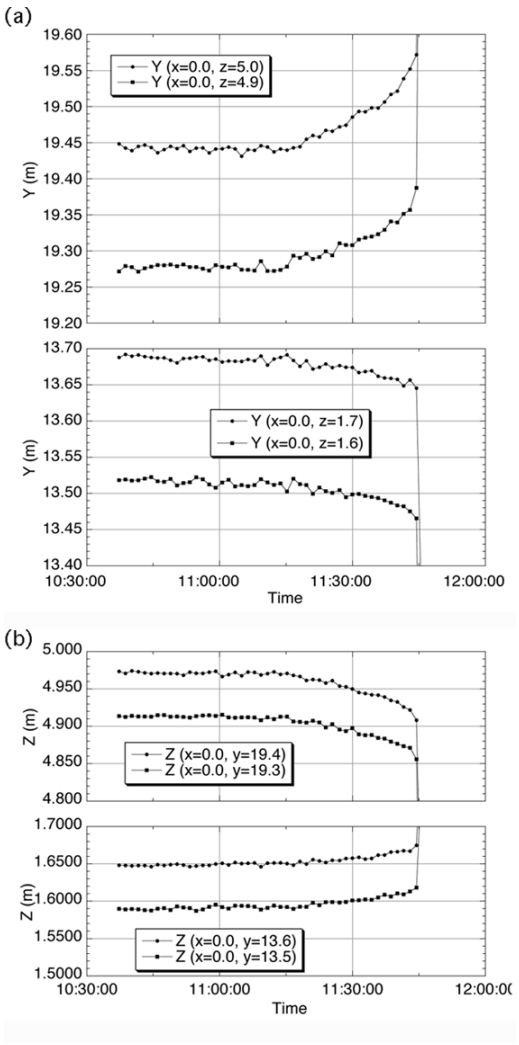

Fig. 8. Time variations in deformation along Y direction (a) and along Z direction (b) in the model slope experiment 2.

Time history of deformation

Figure 7 shows change of longitudinal section of the slope centre (X = 0). In the figure, the deformation amount is enlarged 20 times. In the upper slope, subsidence occurred at the top of the slope before 11:00:36 and extended its area with time. In the lower slope, uplift deformation first appeared around Y = 15, but uplift deformation of the slope between Y = 12.5 and 14 became dominant from 11:19:35. This result indicates a migration of the actively deforming area over time. A similar migration was reported for a landslide in Suemine (1983) and it was considered to result from progressive failure. The mechanism of creep preceding a slope failure is not well understood (Tsuchiya and Ohmura (1985)). This result might provide an incentive for further study of this mechanism.

Figure 8 shows the variations in the grid representative value: (a) shows variations in Y at the grid with values of X and Z, as indicated in the corresponding diagrams; (b) shows those in Z at the grid with values of X and Y, as indicated in the corresponding diagrams. On the uphill grids, retrogression and subsidence appear almost one hour before the failure. The amount of subsidence was up to 0.15 m. Both swelling and uplift are observed on the downhill grids. The amount of deformation is less in downhill grids than that in uphill grids. The final amount of heaving at y = 13.5 was about 0.03 m which is sufficiently large compared to the expected standard deviation. These results show that considerable acceleration in deformation was measurable using this method.

This method provided a two-dimensional aspect of time dependent characteristics of pre-failure deformation of slope such as migration of actively deforming area and acceleration of deformation. Investigation on the characteristics is considered to be important for understanding the mechanism of pre-failure deformation and for developing a more reliable method for failure time prediction. Data that are obtained using this method

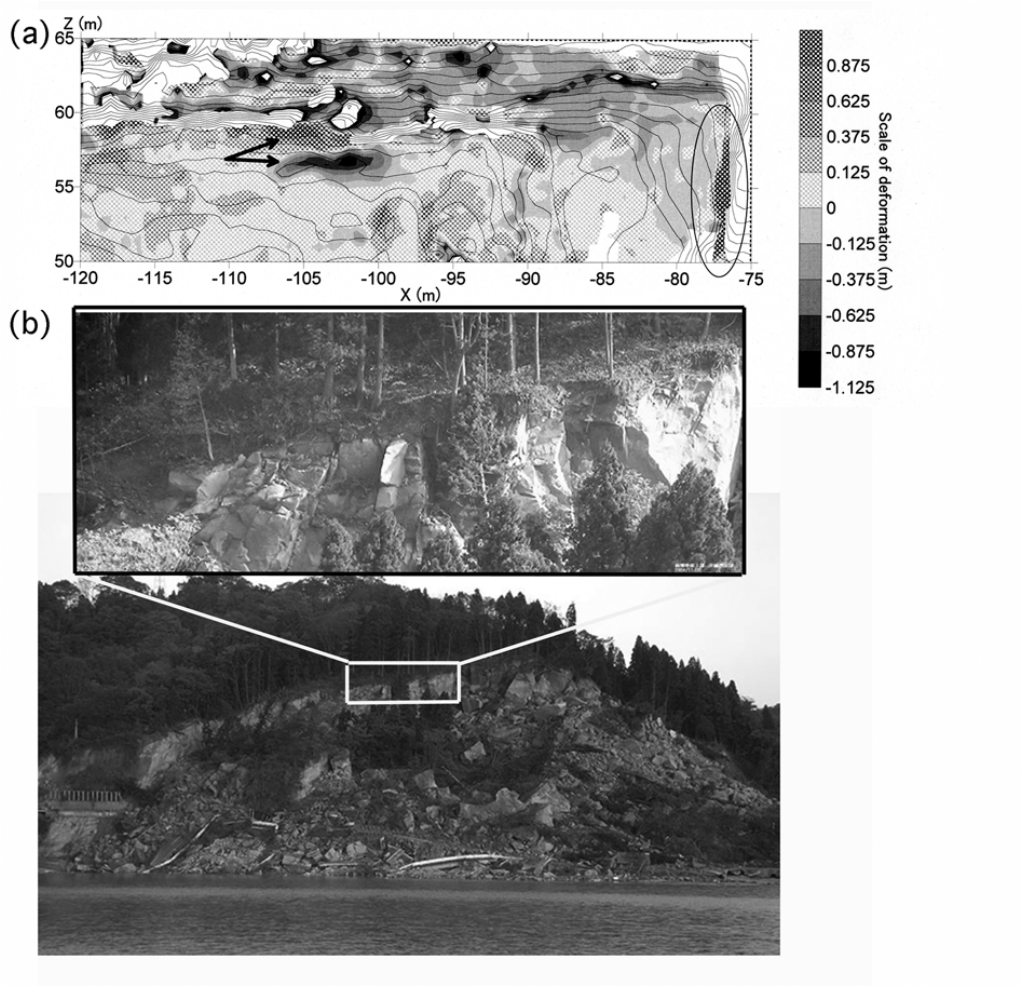

Fig. 9. (a) Distribution of difference in Y between two measurements of scarp of slope failure in Myoken projected on X–Z plane. Solid line indicates contour of Y. (b) Photograph of the failure.

are useful for research as well as for monitoring slope failure.

Application to actual topography

The measurement and analysis techniques were applied to a real slope failure. The scarp of the Myoken failure (Figure 9 (b)) was surveyed by a long-range-type laser scanner on 7 November and 7 December 2004. Though many cracks had been found in the scarp, it could not be watched from the activity site. The author felt necessity of automatic monitoring of it during activity.

The long-range laser scanner was set on the opposite side of the Shinano River. Each measurement took about an hour because of the slow scanning. The time can be reduced by using a high-speed scanner and by setting it nearer location.

Figure 9 (a) shows the difference in Y calculated using 0.5 m mesh between two measurements. The contour line of Y value is shown by the solid line. Areas where data were not obtained due to dead angle caused by trees and topography were masked by white color. Some of them are surrounded by areas of large deformation, for example, an area surrounded by an ellipse ($-77 < \mathrm{X} < -78, 50 < \mathrm{Z} < 60$). These deformations are considered to represent errors that are generated by the fact that low data density causes rough representation of topography resulting that the difference between measurements will be sensitive. Such error can be generated in areas where ground surface is much inclined to the sight line from the scanner, too. To suppress this kind of error, it is necessary to make data density high enough to represent topography precisely. On the other hand, the higher the data density, the longer a measurement takes. It is important to control both the time and the accuracy of measurement when this method is applied to complicated geomorphologies.

A pair of retreat and progress can be seen as indicated by an arrow. According to the photograph, it

corresponds to a rock segmented by a crack. This rock is considered to have shifted slightly during the interval between the two measurements.

Conclusion

In order to estimate the risk of secondary disaster during rescue activities at a site suffering from slope failure, a method was studied for real-time monitoring of slope deformation from a remote location.

The measurement accuracy was determined and spatial stacking was proposed to suppress the effects of measurement error on the calculation of deformations.

Pre-failure surface deformation of the model slope was remotely monitored during an artificial rainfall which eventually caused slope failure. The result revealed the distribution of vertical and horizontal deformations and its variation with time. Subsidence and retrogressing deformations were detected in the uphill area, whereas uplift and swelling deformations were done in the downhill area. Time dependent processes of slope failure were observed, e.g. acceleration in deformation and shift of the actively deforming area. The remote monitoring technique that was used in this study can provide suitable data for understanding the mechanisms of pre-failure slope deformation and for monitoring slope failure.

The measuring and analyzing technique was applied to a scarp of an actual slope failure. Deformation was detected in a rock that had been segmented by cracks. It is clarified that density of data is important to calculate precise deformation in complicated geomorphology. The reliability of monitoring even under such adverse conditions is a topic for further study.

Acknowledgements

The author express his sincere gratitude to Mr. Hiroshi Nagura of the Mathematical Assist Design Lab. Co. Ltd. for his active cooperation throughout this study. The author is grateful to Mr. Fukuzono Teruki, NIED, who provided the opportunity to conduct the model experiments.

References

Ebisawa, T. (2005) On a rescue activity in a slope failure, *Shobo-kenshu 77*, p.144–153.

Fukuzono, T. and Terashima, H. (1985) Experimental study of slope failure in cohesive soils caused by rainfall. *Proc. International Symposium on Erosion, Debris Flow and Disaster Prevention, Tsukuba*, p.346–349.

Fukuzono, T. (1985) A new method for predicting the failure time of a slope. *Proc. 9th Int. Conf. and Field Workshop on Landslides, Tokyo*, p.145–150.

Hayashi, S. and Yamamori, T. (1991) Basic equation of slide in tertiary creep and features of its parameters. *Landslide (Jour. of Japan Landslide Society)*, **28**(1), 17–22.

Nakagawa, A. and Okunishi, K. (1977) A large-scale landslide at Shigeto, Kochi Prefecture — Part 1. Characteristics of ground structure on the landslide. *Bulletin of Disaster Prevention Research Institute of Kyoto University*, **20**(B-1), 209–236 (in Japanese).

Saito, M. and Uezawa, H. (1961) Failure of soil due to creep. *Proc. 5th Int. Conf. on Soil Mechanics and Foundation Engineering, Paris*, 1, p.315–318.

Suemine, A. (1983) Observational study on landslide mechanism in the area of crystalline schist (Part 1) — An example of propagation of Rankine state. *Bulletin of Disaster Prevention Research Institute of Kyoto University*, **33**(3), 105–127.

Tsuchiya, S. and Ohmura, H. (1989) Forecast methods of slope failure time and their case studies. *Landslide (Jour. of Japan Landslide Society)*, **26**(1), 1–8 (in Japanese).

Varnes, D. J. (1982) Time-deformation relations in creep to failure of earth materials. *Proc. 7th Southeast Asian Geotechnical Conf., Hong Kong*, p.107–130.